Optical Nyquist channel generation using a comb-based tunable optical tapped-delay-line

Morteza Ziyadi,[1,*] Mohammad Reza Chitgarha,[1] Amirhossein Mohajerin-Ariaei,[1] Salman Khaleghi,[1] Ahmed Almaiman,[1] Yinwen Cao,[1] Moshe J. Willner,[1] Moshe Tur,[2] Loukas Paraschis,[3] Carsten Langrock,[4] Martin M. Fejer,[4] Joseph D. Touch,[5] and Alan E. Willner[1]

[1]*Department of Electrical Engineering, University of Southern California, Los Angeles 90089, California, USA*

[2]*School of Electrical Engineering, Tel Aviv University, Ramat Aviv 69978, Israel*

[3]*Cisco Systems, San Jose, California 95134, USA*

[4]*Edward L. Ginzton Laboratory, Stanford University, Stanford, California 94305, USA*

[5]*Information Sciences Institute, University of Southern California, Marina del Rey California 90292, USA*

**Corresponding author: ziyadi@usc.edu*

Received September 10, 2014; accepted October 7, 2014;
posted October 22, 2014 (Doc. ID 221795); published November 18, 2014

We demonstrate optical Nyquist channel generation based on a comb-based optical tapped-delay-line. The frequency lines of an optical frequency comb are used as the taps of the optical tapped-delay-line to perform a finite-impulse response (FIR) filter function. A single optical nonlinear element is utilized to multiplex the taps and form the Nyquist signal. The tunablity of the approach over the baud rate and modulation format is shown. Optical signal-to-noise ratio penalty of 2.8 dB is measured for the 11-tap Nyquist filtering of 32-Gbaud QPSK signal.

OCIS codes: (060.2360) Fiber optics links and subsystems; (060.4370) Nonlinear optics, fibers; (190.4223) Nonlinear wave mixing.
http://dx.doi.org/10.1364/OL.39.006585

There has been significant interest in spectrally efficient data channels for optical communication systems [1–4]. In addition to higher-order modulation formats, achieving the minimum bandwidth possible, i.e., the Nyquist bandwidth, optimizes the available spectrum utilization and increases the spectral efficiency measured in bit/s/Hz [5–7].

Several reports have demonstrated Nyquist channels in optical fiber communication systems [5–12]. A common technique to form a Nyquist channel is to use electronic signal processing to shape the data such that the data channel spectrum has a flat top and steeply sloping sides [5,13,14]. In this method, an electronic tapped-delay-line based finite-impulse response (FIR) filter shapes the channel spectrum in the time domain, requiring a digital-to-analog converter (DAC) operating at least twice the baud rate, which is difficult at high baud rates [13,14]. Optical Nyquist pulse sequence generation is one potential approach to achieve the Nyquist channels [6,8–10]. In this approach, Nyquist pulses are generated by filtering the frequency lines of an optical comb source. To achieve a single Nyquist channel, it is desired to have the repetition rate of the pulse sequence to be the same as the pulse width [5], which might be difficult to achieve using the method of optical Nyquist pulse generation [6,8]. Time-division multiplexing (TDM) of different channels could be used to increase the capacity in this approach [6]. Optical channel shaping is another potential approach to achieve the Nyquist channels at high baud rates. Optical wavelength filtering is a common approach to optically generating a Nyquist channel [7,12,14,15]. In this method, the power of the signal at different frequencies is reduced to shape the spectrum in the frequency domain. In contrast to this approach, tapped-delay-line (TDL) FIR filters shape the Nyquist channel by redistributing the channel power into different frequencies [15]. Optically generating a Nyquist channel by operating in the time domain, as does an FIR filter, is thus a desirable goal. Furthermore, such an approach would also be tunable over different high baud rates.

In this Letter, we demonstrate optical Nyquist channel generation for baud rates of 32-and 26-Gbaud as well as binary- and quadrature-phase shift keying (BPSK/QPSK) modulation formats. A comb-based tunable optical tapped-delay-line (OTDL) is used as an FIR filter to shape the optical channels [16–18]. In this approach, the frequency lines of the optical frequency comb source are used as the OTDL taps. A wavelength-dependent delay element is used to delay the signals of different taps. The delayed signals are then coherently multiplexed with the weighted taps in only one nonlinear element. We experimentally generated optical Nyquist QPSK/BPSK signals at 32-Gbaud and 26-Gbaud, demonstrating the tunablity of this approach. The optical signal-to-noise ratio (OSNR) penalties are measured. An OSNR penalty of ~2.8 dB at a bit error rate (BER) of 1e-3 is measured for optical Nyquist QPSK signals generated with 11-taps at 32-Gbaud.

The conceptual block diagram of the Nyquist FIR filter is shown in Fig. 1. The input signal with rectangular pulse shape in the time domain, and hence with a sinc shape ($\mathrm{sinc}(x) = \sin(x)/x$) in the frequency domain, passes through a TDL-FIR filter with appropriate tap coefficients and delays and is converted to a Nyquist signal with a rectangular shape in the frequency domain. The TDL-FIR filter reduces the side lobes of the signal spectrum resulting in better bandwidth efficiency. In order to extract the information from the Nyquist signal, we

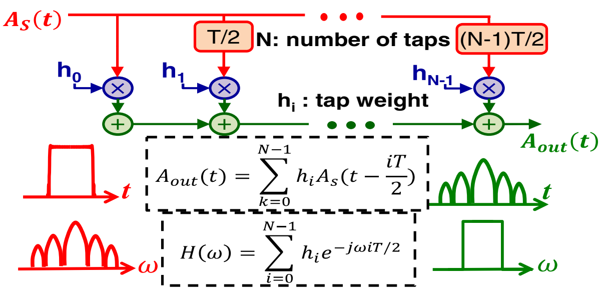

Fig. 1. Concept of Nyquist FIR filter.

synchronize with the sampling time to the peak of the sinc signal. The frequency-comb-based OTDL shown in Fig. 2 implements the TDL-FIR filter in the optical domain to generate a Nyquist signal. This scheme uses a coherent frequency comb source to generate the coherent pump components. Modulating these coherent pumps with the input data stream, $A_S(t)$, generates replicas of the signal at different wavelengths. These replicas are delayed by passing them through a chromatic dispersion element such as a dispersion compensating fiber (DCF). The relative delay between two adjacent replicas is $\Delta\tau = D \cdot \Delta\lambda \cdot L$, where D is the dispersion parameter (ps/nm/km), $\Delta\lambda$ is the wavelength separation (nm) between two pumps, and L is the lengths of the DCF. To realize a Nyquist filter, the delay is set to half of the symbol duration (T), i.e., $T/2$. Different Nyquist channel baud rates can be generated by changing the amount of delay, which here can be obtained by changing the pump-frequency spacing in the comb source or by varying the length of the DCF. The delayed signals with the electrical fields of $A_{s,i}(t) = A_S(t - iT/2)$, $i = 0, 1, \ldots,$ $(N - 1)$ (N = number of taps) equivalent to the optical TDL taps are thus generated. These taps are coherently combined using another set of lines of the frequency-comb source in a periodically poled lithium niobate (PPLN) waveguide with a quasi-phase matching (QPM) frequency of f_{QPM}. Each replica of the signal $A_{s,i}$ at frequency $f_{s,i}$ uses a pump $A_{D,i}$ chosen from the new set of fingers at frequency $f_i = 2f_{\mathrm{QPM}} - f_{s,i}$. Inside the PPLN waveguide in a sum-frequency generation (SFG) process, each pair of the signal and pump generates a new signal at a frequency of $f_i + f_{s,i} = 2f_{\mathrm{QPM}}$ with a value proportional to $A_{s,i}A_{D,i}A_{F,i}$, $i = 0, 1, \ldots, (N - 1)$, where a spatial light modulator (SLM) filter is used to induce arbitrary phase and amplitude on each pump $A_{F,i}$ to adjust the tap coefficients. All generated signals at $2f_{\mathrm{QPM}}$ are coherently combined to result in the signal of $\sum_i (A_{s,i}A_{D,i}A_{F,i})$. By injecting another pump laser, A_P, at f_{pump}, into the PPLN crystal in a difference-frequency-generation (DFG) process, the multiplexed signal at $2f_{\mathrm{QPM}}$ is converted back to the C-band frequency of $f_{\mathrm{out}} = 2f_{\mathrm{QPM}} - f_{\mathrm{pump}}$. Thus, the output is

$$A_{\mathrm{out}}(t) \propto \sum_{i=0}^{N-1} A^*_{\mathrm{pump}} \cdot A_{D,i} \cdot A_{F,i} \cdot A_S\left(t - \frac{iT}{2}\right), \qquad (1)$$

in which A^*_{pump} is the complex conjugate of the electrical field of the pump signal. Assuming $h_i = A^*_{\mathrm{pump}} \cdot A_{D,i} \cdot A_{F,i}$, the output becomes

$$A_{\mathrm{out}}(t) \propto \sum_{i=0}^{N-1} h_i A_S\left(t - \frac{iT}{2}\right), \qquad (2)$$

which is the same as the FIR filter equation.

The experimental setup is shown in Fig. 3. A mode-locked laser (MLL) with a 10-GHz repetition rate and 2-ps pulse width is used as a comb source. The frequency spacing between the lines is increased using a delay-line interferometer (DLI) with a free spectral range of 20-GHz. The resulting frequency comb is sent through a highly nonlinear fiber (HNLF) to generate a flat and broad spectrum. An SLM filter is used to select two sets of the frequency lines for the signal and pump path. The SLM is also used to apply complex weights on the pumps. For each path, up to 11 comb lines with a frequency spacing of 120-GHz are selected. In the signal path, after preamplification, a nested Mach–Zehnder modulator modulates the 32-Gbaud (and 26-Gbaud) QPSK (BPSK) data (PRBS $2^{31} - 1$) on the comb components. The signals are amplified in an erbium-doped fiber amplifier (EDFA) and travel through a ~200 m (and 250-m) DCF. The amplified frequency pump lines from the coherent pumps path and another amplified laser pump at ~1564 nm are sent through the same DCF to increase stability. All the signals and pumps are injected into a 4-cm-long PPLN waveguide with the temperature tuned QPM wavelength of ~1550.5 nm to create the final Nyquist channel with the spectrum shown. The OSNR of ~35 dB could be achieved for the generated Nyquist signal, which could be potentially improved if one can use a waveguide with higher conversion efficiency. We

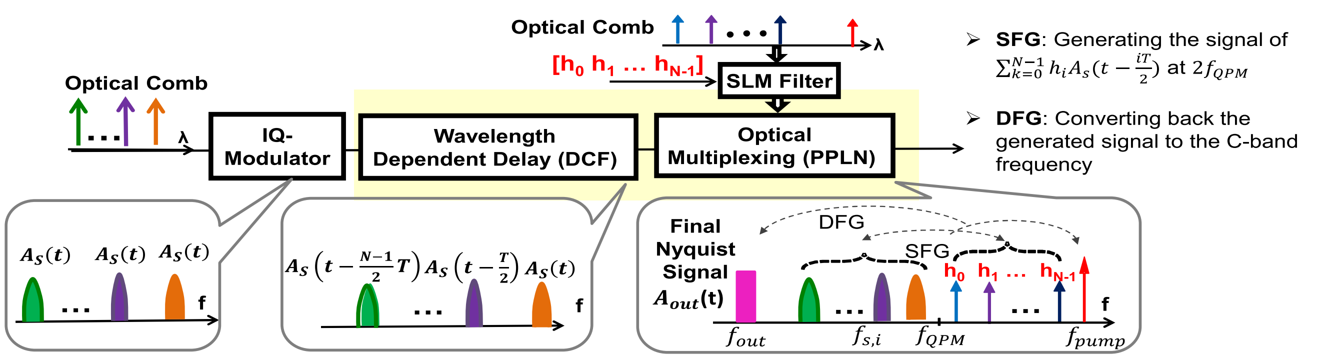

Fig. 2. Concept of optical Nyquist signal generation using comb-based OTDL (an optical comb as the taps of the FIR filter and DCF to delay the tapped signals and a PPLN waveguide to multiplex the tapped delayed signals).

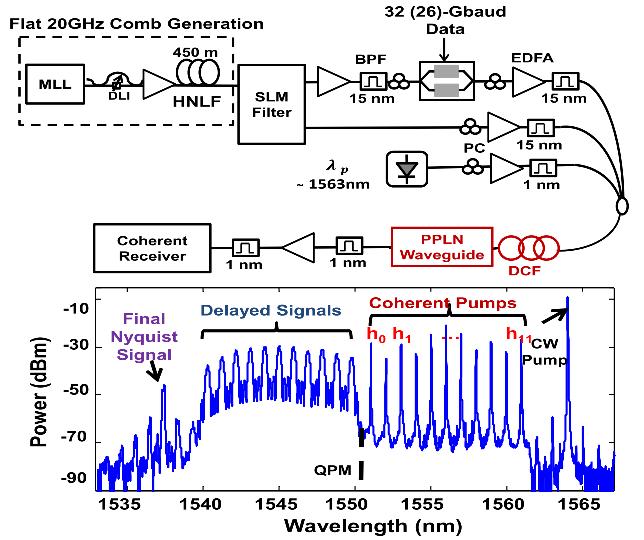

Fig. 3. Experimental setup for the optical Nyquist channel generation. BPF, bandpass filter; PC, polarization controller.

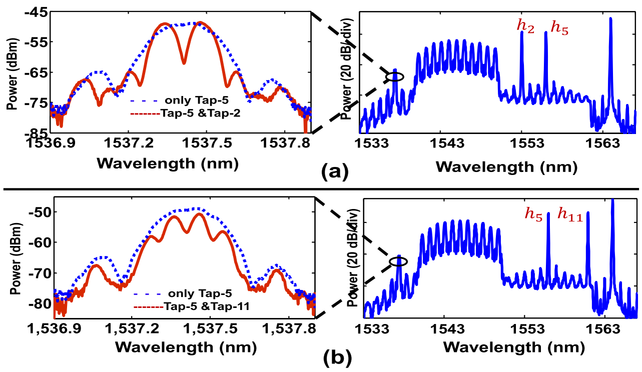

Fig. 4. Experimental results for the calibration of taps. (a) Tap-2 calibration. (b) Tap-11 calibration.

calibrate the tap weights to the appropriate values with the central tap ($i = N/2$ where x means the floor of x) selected as the reference tap. In order to calibrate the tap-k coefficient, we set the coefficients as $h_i = 1$ for $i = k$, $N/2$ and $h_i = 0$ for $i \neq k$, $N/2$. In order to set a coefficient to 0, we turn off the corresponding pump. To tune a coefficient to 1, we tune the amplitude and phase of the corresponding pump in the SLM filter to achieve a symmetric shape at the output spectrum. For instance, Fig. 4 shows the experimental results on the calibration for the taps of 2 and 11. As shown in Fig. 4(a) (right) only two pumps corresponding to the taps of 5 (central tap) and 2 (calibrated tap) are on and the rest of the pumps are off. After adjusting the tap-2 coefficient to 1, the output signal spectrum in Fig. 4(a) (left) is obtained compared to the input signal spectrum in the figure. In Fig. 4(b), the calibration of tap 11 is shown. After calibrating all the taps, the amplitude and phase of the taps are adjusted to the Nyquist-filter tap weights. Figure 5 shows the simulation and experimental results. Figure 5(a) shows the simulation and experimental results of the Nyquist filter shape and Nyquist signal spectrum for 32-Gbaud signals. The experimental results match the simulation. In order to show baud-rate tunability, we implement a 26-Gbaud Nyquist signal generation. The setup is adjusted to generate a 26-Gbaud Nyquist channel by replacing a 200-m DCF (for the 32-Gbaud experiment) with a 250-m DCF. The results for 26-Gbaud Nyquist signal generation are shown in Fig. 5(b). As shown, increasing the number of taps can shrink the generated signal bandwidth to the Nyquist bandwidth and flatten the top of the input signal. Furthermore, we analyze the generated signal quality in terms of the error vector magnitude (EVM) and BER measured by commercially available Agilent Technologies digital signal analyzer (DSA)-X 93204A. An EVM of 20% at 32-Gbaud for the 11-tap Nyquist QPSK signal is measured, which is compared to the input QPSK signal EVM of 13% [Fig. 6(a)]. In Fig. 6(a), the BER curves for different numbers of taps show the degradation as OSNR penalties. An OSNR penalty of 2.8 dB at BER of 1e-3 is achieved for the 11-tap filter. Similar results are shown for 26-Gbaud Nyquist QPSK signal generation [Fig. 6(b)]. Figure 6(c) shows the OSNR penalty versus number of taps, as well as bandwidth efficiency. We plot the bandwidth efficiency as the bandwidth between the main ripples on

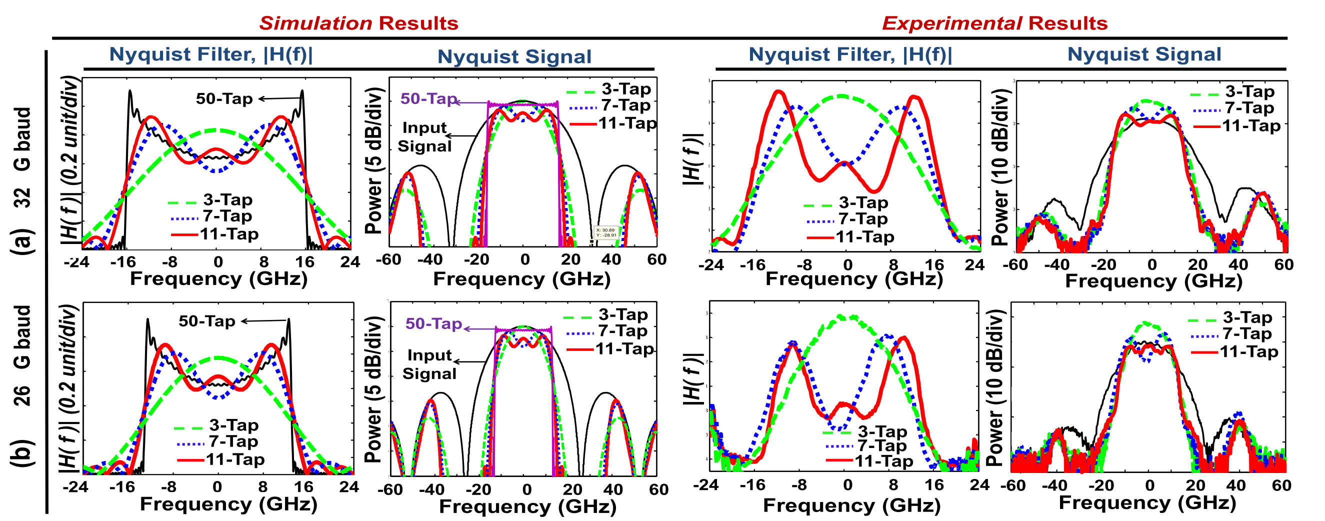

Fig. 5. Results of Nyquist filter shape, i.e., $|H(f)|$, and Nyquist signal spectrum for different number of taps at (a) 32-Gbaud and (b) 26-Gbaud. Experimental results match the simulation results.

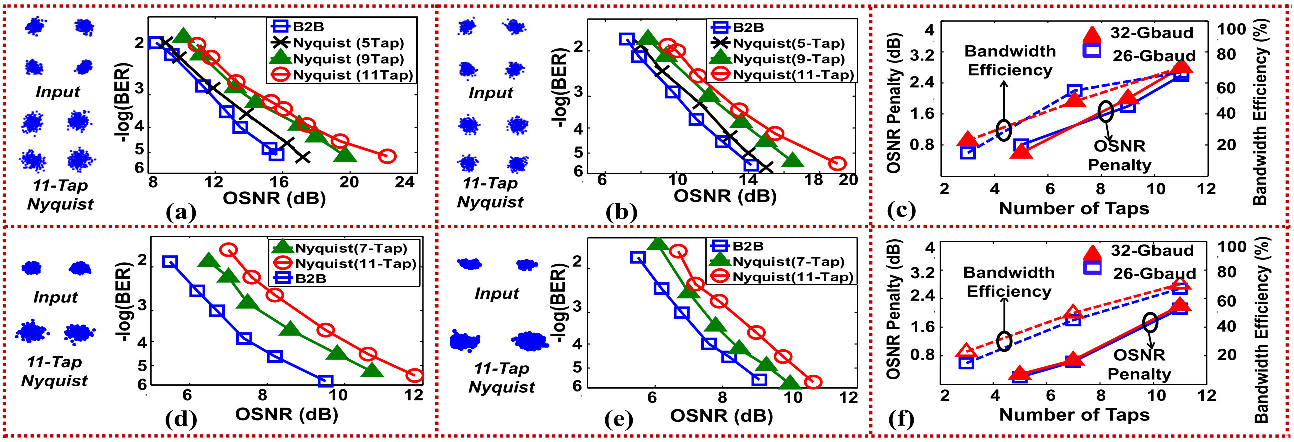

Fig. 6. Experimental results. (a), (b) Constellation and BER measurements versus OSNR of 32-Gbaud (a) and 26-Gbaud (b) QPSK signal. (c) Measured OSNR penalty and bandwidth efficiency versus number of taps for QPSK signals. (d), (e) BER measurements of 32-Gbaud (d) and 26-Gbaud (e) BPSK signal. (f) Measured OSNR penalty of BPSK signals.

the Nyquist signal spectrum divided by the ideal Nyquist bandwidth. This figure shows the trade-off between the OSNR penalty and bandwidth efficiency. Finally, we generate the Nyquist BPSK signals at two baud rates of 32- and 26-Gbaud. Similar results are obtained in terms of the Nyquist filter shape and Nyquist signal spectrum. The BER and EVM measurements are shown in Figs. 6(d), and 6(e) for Nyquist BPSK signals. Figure 6(f) shows the OSNR penalty and bandwidth efficiency measurements for the case of Nyquist BPSK signal generation. To conclude, we could generate the Nyquist channel at high baud rates by implementing a comb-based OTDL-FIR filter. Although we just implemented the Nyquist channel generation for a single polarization, it might be possible to extend it to dual-polarized signals using a polarization diversity loop structure.

This work was made possible by the support from NSF and Center for Integrated Access Networks.

References

1. P. J. Winzer and R.-J. Essiambre, J. Lightwave Technol. **24**, 4711 (2006).
2. R. D. J. Filling, Science **330**, 327 (2010).
3. S. Chandrasekhar and X. Liu, J. Lightwave Technol. **30**, 3816 (2012).
4. J.-X. Cai, J. Lightwave Technol. **30**, 3845 (2012).
5. R. Schmogrow, M. Winter, M. Meyer, D. Hillerkuss, S. Wolf, B. Baeuerle, A. Ludwig, B. Nebendahl, S. Ben-Ezra, J. Meyer, M. Dreschmann, M. Huebner, J. Becker, C. Koos, W. Freude, and J. Leuthold, Opt. Express **20**, 317 (2012).
6. J. Zhang, J. Yu, Y. Fang, and N. Chi, Sci. Rep. **4**, 6156 (2014).
7. Y. Huang, D. Qian, F. Yaman, T. Wang, E. Mateo, T. Inoue, Y. Inada, Y. Toyota, T. Ogata, M. Sato, Y. Aono, and T. Tajima, in *Optical Fiber Communication Conference* (Optical Society of America, 2013), paper NW4E.1.
8. T. Hirooka, P. Ruan, P. Guan, and M. Nakazawa, Opt. Express **20**, 15001 (2012).
9. M. A. Soto, M. Alem, M. A. Shoaie, A. Vedadi, C.-S. Brès, L. Thévenaz, and T. Schneider, Nat. Commun. **4**, 2898 (2013).
10. S. Preussler, N. Wenzel, and T. Schneider, IEEE Photon. J. **6**, 1 (2014).
11. X. Zhou and L. E. Nelson, J. Lightwave Technol. **30**, 3779 (2012).
12. G. Bosco, V. Curri, A. Carena, P. Poggiolini, and F. Forghieri, J. Lightwave Technol., **29**, 53 (2011).
13. J. Wang, C. Xie, and Z. Pan, J. Lightwave Technol., **30**, 3679 (2012).
14. G. Bosco, in *Optical Fiber Communication Conference* (Optical Society of America, 2012), paper OM3H.1.
15. A. Ghazisaeidi, P. Tran, P. Brindel, O. Bertran-Pardo, J. Renaudier, G. Charlet, and S. Bigo, in *Optical Fiber Communication Conference* (Optical Society of America, 2013), paper OTu3B.6.
16. M. Ziyadi, M. R. Chitgarha, S. Khaleghi, A. Mohajerin-Ariaei, A. Almaiman, J. Touch, M. Tur, C. Langrock, M. M. Fejer, and A. E. Willner, Opt. Express **22**, 84 (2014).
17. S. Khaleghi, O. F. Yilmaz, M. R. Chitgarha, M. Tur, N. Ahmed, S. R. Nuccio, I. M. Fazal, X. Wu, M. W. Haney, C. Langrock, M. M. Fejer, and A. E. Willner, IEEE Photon. J. **4**, 1220 (2012).
18. M. Ziyadi, M. R. Chitgarha, A. Mohajerin Ariaei, S. Khaleghi, A. Almaiman, M. Willner, J. Touch, M. Tur, L. Paraschis, C. Langrock, M. Fejer, and A. Willner, in *Optical Fiber Communication Conference* (Optical Society of America, 2014), paper W1G.2.